Correlated quantization of supercurrent and conductance in a superconducting quantum point contact

T. Bauch,* E. Hürfeld, V. M. Krasnov, and P. Delsing
Microtechnology and Nanoscience, MC2, Chalmers University of Technology, S-412 96 Göteborg, Sweden

H. Takayanagi and T. Akazaki
NTT Basic Research Laboratories, 3-1 Morinosato-Wakamiya, Atsugi-Shi, Kanagawa 243-01, Japan
(Received 10 May 2004; revised manuscript received 11 October 2004; published 3 May 2005)

We have measured the supercurrent and conductance of a superconducting quantum point contact in a superconductor two-dimensional electron gas-superconductor Josephson junction. We observe that the supercurrent and conductance change stepwise in a correlated manner as a function of the gate voltage. This was achieved by simultaneous measurement of the supercurrent and conductance at high bias from the same current voltage characteristic.

DOI: 10.1103/PhysRevB.71.174502 PACS number(s): 74.45.+c, 74.50.+r, 74.78.Fk, 72.20.Jv

I. INTRODUCTION

In analogy with the quantized conductance of a normal conducting quantum point contact (QPC)[1,2] a quantization of the supercurrent is expected to be observable in a superconducting quantum point contact (SQPC).[3–7] This results from the quantization of the transverse momentum of the quasiparticles in the QPC constriction with a width of the order of the Fermi wavelength λ_F. The number of transport modes is given by $2W_g/\lambda_F$, where W_g is the constriction width. Each transport mode contributes one quantized conductance unit $\Delta G_0 = 2e^2/h$ to the total conductance and one quantized supercurrent unit ΔI_{C0} to the critical current of the SQPC. Here e is the electron charge and h the Planck constant. In the limit of a short junction where the length of the junction L is much smaller than the superconducting coherence length ξ_0 a stepwise change of the supercurrent and conductance was observed in a mechanically controllable break junction.[8]

The first indication of the critical current quantization in the limit of a long junction, $L \geqslant \xi_0$, was obtained in Ref. 9 for a ballistic superconductor two-dimensional electron gas-superconductor (S-2DEG-S) Josephson junction. Here the constriction in the 2DEG was created by applying a voltage to the split gate. A stepwise change of the critical current I_c and the conductance G could be observed by varying the gate voltage of the split gate. Surprisingly the position of the critical current step was different from that of the corresponding conductance step. The present theory predicts an agreement between the position of the conductance and supercurrent steps.

In this paper we present new experimental data for a SQPC in a S-2DEG-S Josephson junction. We measured the current voltage characteristic (IVC) for different gate voltages V_g. This way we were able to determine simultaneously the critical current and conductance along the same IVC. Unlike the previous work[9] in which a correlation between the conductance and the critical current was not observed, our data show that the critical current and conductance steps appear at the same gate voltages. In addition we observe the onset of the first transport mode contributing both to the supercurrent and the conductance of the SQPC. The amplitude of the critical current steps is in agreement with theoretical estimations, even though for small values of I_C the critical current step height is reduced by thermal fluctuations.

II. THEORY

It is well known that the critical supercurrent I_C of a classical Josephson point contact is directly related to its conductance G and is given by $\pi G\Delta_0/e$,[10] where Δ_0 is the energy gap of the superconductor. The same holds for a SQPC. The conductance of a QPC is given by the well known Landauer Büttiker formula[11,12]

$$G = \frac{2e^2}{h}\sum_{n=1}^{N} T_n, \tag{1}$$

where $N = 2W_g/\lambda_F$ is the maximum number of the 1D transport modes in the quantum point contact and $n \leqslant N$ is the index for each transport mode. The transmission coefficient for the nth transport mode is given by T_n. The transmission probability T_n depends on the form of the potential barrier at the constriction. In the adiabatic case it can be approximated by $V_x(x) = V_0 - m^*\omega_x^2 x^2/2$, and the transmission coefficient takes the form

$$T_n = \frac{D_n}{1 + \exp\left(-2\pi\dfrac{E_F - E_n - V_0}{\hbar\omega_x}\right)}, \tag{2}$$

where E_F is the Fermi energy and E_n are the 1D sublevel energies in the transverse potential $V_y(y)$ at the saddle point of the constriction. D_n takes the scattering at impurities into account. $1/\omega_x$ describes the "sharpness" of the steps. From Eq. (2) for an open channel it follows that $T_n = D_n$. In the case of ballistic electron transport in the quantum point contact all transport modes with $n \leqslant N$ are completely open, $T_n = 1$. Each open transport mode contributes the quantized conductance $\Delta G_0 = 2e^2/h$ to the total conductance,

$$G = N\frac{2e^2}{h} = N\Delta G_0. \tag{3}$$

According to Eq. (3) the conductance changes stepwise with step height ΔG_0 as a function of the width of the constriction as the maximum number of transport modes $N = 2W_g/\lambda_F$, which is an integer, depends on the constriction width. One has to point out that the conductance quantum ΔG_0 does not depend on the geometry of the conductor.

First we assume an ideal interface between the superconductor and the normal conductor, i.e., there is no potential barrier at the interface. In accordance with Ref. 13 we will use the factor Z to describe the barrier strength. Z is related to the transmission probability D_Z of the interface barrier by $D_Z = 1/(1+Z^2)$. In the case of a short SQPC ($\xi_0 \gg L$) and $Z = 0$ the supercurrent is given by[3]

$$I_C = N\frac{2e^2}{h}\frac{\pi\Delta_0}{e} = G\frac{\pi\Delta_0}{e}. \tag{4}$$

All N transport modes carry the quantized supercurrent $\Delta I_{C0} = e\Delta_0/\hbar$ which does not depend on the junction geometry. As for the conductance the supercurrent changes stepwise as a function of the width of the constriction.

In the opposite case of a long ballistic SQPC ($L \geqslant \xi_0$) the Josephson current flows via many bound states and the quantization of the supercurrent is not anymore universal but depends on junction parameters.[5] The ratio L/ξ_0 gives roughly the number of Andreev bound states within the energy gap Δ_0 which carry the Josephson current.[5] In this case and assuming no barrier potential at the interface ($Z=0$), the supercurrent is quantized in units of $e/(\tau_0 + \hbar/\Delta_0)$.[6] Here τ_0 is the time of flight a quasiparticle requires to traverse the normal region of length L. During the time $\hbar/\Delta_0$ an electron wave packet is Andreev reflected into a hole wave packet. For a completely open transport mode the travel time can be approximated by $\tau_0 = L/v_F$ and the supercurrent quantization saturates at the nonuniversal value[6]

$$\Delta I_{C0} = \frac{ev_F}{L + \pi\xi_0}. \tag{5}$$

In contrast to the supercurrent quantization in the short junction limit ($\xi_0 \gg L$) [Eq. (4)], the supercurrent quantization in the long junction limit ($L \geqslant \xi_0$) depends both on the Fermi velocity v_F and the junction length L of the normal conducting region.

A finite barrier potential at the interface between the superconductor and normal conductor ($Z > 0$) and a Fermi velocity mismatch will further decrease the probability of Andreev reflection and increase the probability of normal reflection.[13] This will influence both the conductance and the supercurrent quantization. In the case of the conductance, a quasiparticle which traveled through the constriction will have a finite probability to be reflected at the normal conductor/superconductor interface and backscattered through the constriction in the opposite direction. This results in a transmission probability T_n in Eq. (1) smaller than 1 even if the transport through the constriction itself is purely ballistic. Consequently the conductance quantization will not have the universal value $2e^2/h$ and the conductance as a function of the constriction width will have step heights, depending on the random transmission probabilities T_n. The effect of reduced Andreev probability will be a reduction of the supercurrent through the constriction and consequently a reduction of the quantization of the supercurrent.[5–7] According to Ref. 7 the supercurrent step height in the presence of scattering is given by

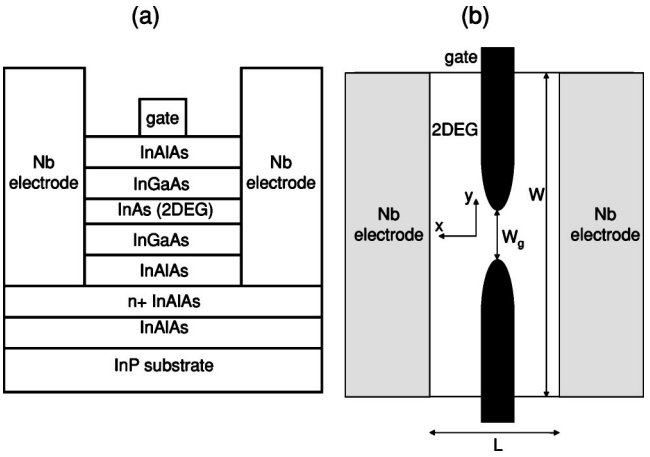

FIG. 1. (a) Cross sectional view of the superconducting quantum point contact (SQPC). The carrier concentration n_S in the 2DEG can be varied by applying a voltage to the gate electrode. (b) Top view of the SQPC. The width of the sample is $W = 10\ \mu$m, the length $L = 400$ nm, and the width between the two gate electrodes is $W_g = 100$ nm.

$$\Delta I_{Cn} = \frac{T_n}{4\pi}\frac{e}{\tau}, \tag{6}$$

with

$$\tau = \frac{\hbar}{\Delta_0} + \tau_0\left(\frac{2}{D_n} - 1\right). \tag{7}$$

III. SAMPLE

The schematic cross section and the top view of the sample is shown in Fig. 1. The 2DEG is localized in a 4 nm thick InAs layer inserted in an $In_{0.52}Al_{0.48}As/In_{0.53}Ga_{0.47}As$ heterostructure grown by molecular beam epitaxy on a Fe doped semi-insulating InP substrate. The two 100 nm thick Nb electrodes, which are coupled to the 2DEG, were defined by the lift off process and electron beam lithography. InAs was used as it does not form a Schottky barrier at the interface to the niobium electrodes which does GaAs. Details of the fabrication process are reported elsewhere.[14] The distance between the Nb electrodes is $L = 400$ nm and the total width of the junction is $W = 10\ \mu$m. Shubnikov-de Haas measurements[9] of the 2DEG at 4.2 K on similar samples give the sheet carrier concentration $n_S = 2.3 \times 10^{12}$ cm^{-2}, the mobility $\mu = 1.11 \times 10^5$ cm^2/V s and the effective mass $m^* = 0.045 m_e$, where m_e is the free electron mass. This results in a Fermi velocity $v_F = \sqrt{2\pi\hbar^2 n_S/m^{*2}} = 9.8 \times 10^5$ m/s and elastic scattering time $\tau = \mu m^*/e = 2.84 \times 10^{-12}$ s, where e is the

electron charge. From these values the mean free path $l = v_F\tau = 2.8$ μm and the normal coherence length in the clean limit $\xi_N = \hbar v_F / 2\pi k_B T = 0.28$ μm at 4.2 K are calculated. The Fermi wavelength is $\lambda_F = \sqrt{2\pi / n_S} = 16.5$ nm.

The length of the Al split gate is 100 nm and the distance between the two gate electrodes is $W_g = 100$ nm. By applying a gate voltage $V_g \simeq -1$ V the 2DEG under the gate electrodes is depleted. In this case the current is flowing only within the constriction between the two gate electrodes. Going to more negative gate voltages $V_g < -1$ V will further deplete the 2DEG within the constriction, reducing the width of the constriction W_g. Finally, at gate voltages $V_g < -2.1$ V, the 2DEG within the constriction is completely pinched off.

The Nb electrodes have a superconducting transition temperature of about 6 K which results in an energy gap $\Delta_0 \simeq 0.9$ meV. This gives us for the superconducting coherence length in the 2DEG $\xi_0 = \hbar v_F / \pi\Delta_0 = 230$ nm where v_F is the Fermi velocity in the 2DEG. Therefore the junction is in the ballistic ($l > L$) and long junction ($L \geqslant \xi_0$) regime and in the clean limit ($\xi_N < l$).

At a temperature of 25 mK and at zero gate voltage the junction under investigation has a critical current $I_{C0} = 8.5$ μA and a normal state resistance $R_N = 38$ Ω.

IV. MEASUREMENTS

The measurements were performed in a ^{3}He-^{4}He dilution refrigerator with a base temperature of 15 mK. To protect the sample from external noise and from 4 K photons, the electrical lines to the sample in the cryostat are well filtered. At the 1 K pot, a home-built RCL filter[15] with a cutoff frequency of 100 MHz is installed. At the mixing chamber a combination of two meters Thermocoax[16] plus a home-built copper-powder filter is installed with a cutoff frequency of 1 GHz. Magnetic shielding of the sample is provided by two Cryoperm shields inside the cryostat and one μ-metal shield outside the cryostat.

In order to analyze the gate voltage dependence of the conductance and critical current of the SQPC, we measured the current voltage characteristics (IVC) at different gate voltages. This allows us a simultaneous determination of the critical current I_C and conductance G_{IVC} from the same IVC. In a second measurement run (the sample was warmed up and cooled down again in order to remove the magnetic shields), we measured the differential zero bias conductance G_{ac} with an applied magnetic field to suppress the critical current, as was done in Ref. 9.

The current voltage characteristics of the SQPC were recorded using a standard four point measurement technique. For each gate voltage we recorded 50 IVCs. The IVC for three different gate voltages at $T = 25$ mK are shown in Fig. 2. For increasing absolute value of the gate voltage $|V_g|$ the supercurrent is decreasing. For gate voltages $V_g < -1.8$ V, the supercurrent branch in the current voltage characterisics shows a finite resistance as shown in the inset of Fig. 2. This can be attributed to thermal smearing of the current voltage characteristic,[17] as the Josephson energy $E_J / k_B = I_C \Phi_0 / 2\pi k_B$ in this gate voltage range is of the order of the bath temperature. Here $\Phi_0 = h/2e$ is the superconducting flux quantum and k_B the Boltzmann constant.

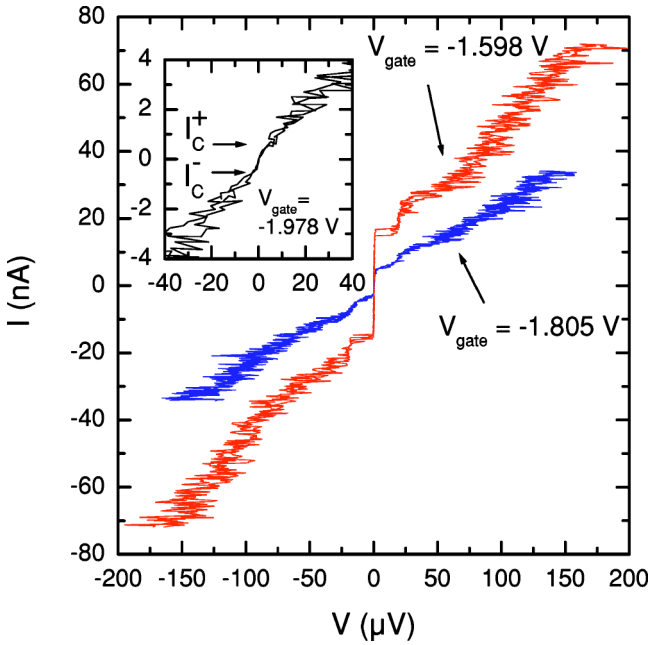

FIG. 2. Measured current voltage characteristics (IVC) at $T = 25$ mK for different gate voltages. In the inset the arrows indicate the onset of the positive I_C^+ and negative I_C^- critical current at $V_{gate} = -1.978$ V which is carried by the first open transport mode.

From the measured IVCs we extracted the critical current and the conductance. The critical current was determined by using a threshold voltage of 3 μV. This still allows us to extract a critical current from the IVC for gate voltages $V_g < -1.8$ V (see the inset of Fig. 2). From the same IVC the conductance is obtained by fitting the resistive branch in the voltage range between 100 μV and 150 μV. In this voltage range the IVC is linear and does not show any structure. Here we have to point out that the conductance extracted for voltages smaller than $2\Delta/e$ might be enhanced by Andreev reflection.[9] For voltages larger than $2\Delta/e$, where the conductance is not affected by Andreev reflection, the measured conductance does not show any step structure as a function of gate voltage. Instead it shows only a linear dependence which was also observed in Ref. 9. We attribute this effect to heating of the 2DEG at high bias voltages, which smears out the step structure of the conductance as a function of the gate voltage.

The averaged critical current and conductance values, which were extracted from 50 IVCs at each gate voltage, are shown in Fig. 3 in the gate voltage range -2.1 V $< V_g < -1.4$ V. For comparison, also, the differential zero bias conductance G_{ac} is shown in Fig. 3(a) with an added offset of $2e^2/h$ for clarity. G_{ac} was measured at a magnetic field of 200 mT to suppress any contribution of Andreev reflection to the conductance. The differential conductance was measured with an AC excitation current $I_{AC} = 10$ nA. To check for nonlinearities possibly due to a residual Josephson current or Andreev reflection in the current voltage characteristics at a magnetic field of 200 mT we varied the AC excitation current from 5 nA to 50 nA which results in a voltage drop across the junction from 90 μV to 900 μV at $V_g = -1.98$ V and from 11 μV to 110 μV at $V_g = -1.2$ V. No

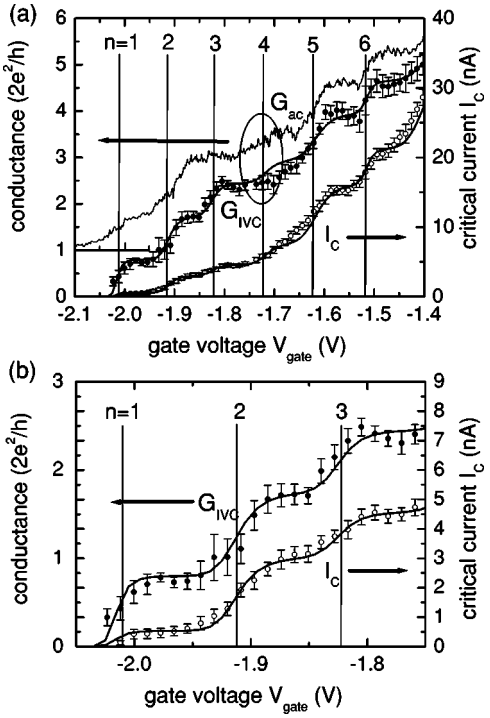

FIG. 3. (a) Critical current I_C (open symbols) and conductance G_{IVC} (full symbols) extracted from the current-voltage characteristics as a function of the gate voltage V_g at $T=25$ mK. The solid lines are fits (for details see the text). The mode number is indicated by an n. The upper curve is the differential zero bias conductance G_{ac} measured at 200 mT which has been shifted by $2e^2/h$ for clarity. (b) A closeup of the critical current I_C (open symbols) and conductance G_{IVC} (full symbols) extracted from the current-voltage characteristics. Solid lines are fits (for details see the text).

difference within the measurement accuracy between the differential conductances as a function of the gate voltage for the different excitation currents was observed. Herewith we can rule out any influence of Andreev reflection on the measured zero bias conductance.

In Fig. 3 one can clearly see that both the conductance G_{IVC} and the critical current I_C extracted from the IVC and the differential zero bias conductance G_{ac} change stepwise as a function of the gate voltage V_g. The difference in the step structure between the conductance G_{IVC} extracted from the IVC and the differential zero bias conductance G_{ac} can be attributed to a reconfiguration of the scattering centers in the SQPC between the two measurement runs. Between the measurements the sample was warmed up to room temperature to remove the cold magnetic shields. This makes a comparison between the gate voltage dependence G_{ac} and I_C difficult, as the reorganization of the scattering centers influences the transmission probabilities T_n.

In the following we will only analyze and compare the gate voltage dependence of the conductance G_{IVC} and critical current I_C, as they have been determined simultaneously from the same IVCs. In Fig. 3 the appearance of the steps are marked with the index n which corresponds also to the transport mode index contributing both to the conductance and the critical current. The steps ($n=1$, 2, 3, 5, 6) in the conductance are also seen as steps in the critical current. This shows

TABLE I. Fitting parameters for the conductance G_{IVC} and critical current I_C (see the text).

Channel	1	2	3	4	5	6
D_n	0.80	0.95	0.70	0.50	1.00	0.70
$\frac{-2\pi(E_F-V_0)}{\hbar\omega_x}$	10	10	15	15	15	40
k_{corr}	1.00	0.98	1.03	1.00	1.00	1.00
τ_0 (ps)	12	3.5	3.0	0.45	0.76	0.65

the correlation between the critical current and the conductance. Only at the gate voltage $V_g=-1.725$ V where the fourth step is expected, no step is seen in the conductance and supercurrent data (see Fig. 3). In particular one can see that as soon as the first ($n=1$) transport mode contributes to the first conductance step at a gate voltage $V_g=-2.02$ V it also contributes to the first critical current step with a step height $\Delta I_C=0.5$ nA [see Fig. 3(b)]. The current voltage characteristic for $V_g=-1.978$ V, corresponding to the first open channel is shown in the inset of Fig. 2. We can rule out that the extracted critical current for the first step ($n=1$) is only due to the choice of the threshold voltage $V_t=3$ μV and the conductance. The contribution of the threshold voltage to the extracted critical current is $\Delta I=GV_t\simeq 160$ pA for the first step ($n=1$). This is about 32% of the total extracted current. For all other steps the contribution of the threshold voltage to the extracted critical current is less than 10%.

V. DISCUSSION

Following Chtchelkatchev[6] (or Shchelkachev[7]) we fitted the conductance G_{IVC} extracted from the IVC using Eqs. (1) and (2). The 1D sublevel energies are parametrized as $E_n=(E_F-V_0)n^2/(k_Gk_{corr})^2$. k_G is the parameter that controls the opening of the channels and is assumed to depend linearly on the gate voltage. The correction factor k_{corr} is introduced to adjust for a shift of the onset of the steps in relation to the gate voltage. The fitting parameters D_n, k_{corr} and $-2\pi(E_F-V_0)/\hbar\omega_x$ are shown in Table I. Using this set of fitting parameters extracted from the conductance, we also fitted the supercurrent according to Eq. (6). Here the only fitting parameter is the classical time of flight τ_0 of the quasiparticles, which is shown in Table I. The time of flight τ_0 influences only the step height of the critical current, but not its position on the gate voltage axis. The fitted graphs for the conductance G_{IVC} and critical current I_C are shown in Fig. 3.

From Table I we see that the steps in the conductance and critical current appear at almost equidistant gate voltage intervals, as the correction factor k_{corr} is practically 1 for all steps. Furthermore the "sharpness" of the steps, which is given by $-2\pi(E_F-V_0)/\hbar\omega_x$, is of the same order of magnitude for all the steps. The average transmission probability extracted from Table I is $D_{eff}=0.775$. This can be attributed to the finite barrier potential at the 2DEG-Nb interface. A rough estimate[18] of the barrier strength Z at the interface can be derived from the relation $R_N=R_{Sh}(1+2Z^2)$ where $R_N=38$ Ω is the resistance of the SQPC at zero gate voltage and

R_{Sh} the Sharvin resistance $R_{Sh}=(h/2e^2)(\lambda_F/2W)$. With $W=10\ \mu$m and $\lambda_F=16.5$ nm we get for the Sharvin resistance $R_{Sh}=10.7\ \Omega$ which results in a barrier strength $Z=1.1$ or transmission probability $D_Z=0.45$. The reason for D_Z being smaller than D_{eff} can be attributed to the inhomogeneity along the 2DEG-Nb interface which will result in a varying transmission probability along the interface. D_Z is an average transmission probability along the junction width $W=10\ \mu$m and D_{eff} is a local measure of the transmission probability on the length scale of the constriction width $W_g=100$ nm which can differ substantially from D_Z. Another reason could be that the conductance in the bias voltage range between 100 μV and 150 μV is still slightly affected by Andreev reflection at the 2DEG/Nb interface.[9]

The height of the steps of the supercurrent I_C as a function of gate voltage V_g in Fig. 3 depends on the gate voltage. The step height increases for increasing step number. This effect is reflected in the fitted values for the time of flight τ_0 (see Table I). The step height for $n\leqslant 3$ is smaller than 2 nA which could be attributed to a reduced measured critical current due to spurious noise in the measurement setup and thermal fluctuations. The Josephson energy of a junction with a critical current of 1 nA corresponds to a temperature of 24 mK, which is the bath temperature of our experiment. For steps $n=5$ and $n=6$ we have a step height of $\Delta I_c\simeq 5$ nA. The respective time of flights are smaller than 1 ps and are in agreement with the expected value $\tau_0\simeq L/v_F=0.4$ ps.

From the critical current at zero gate voltage $I_{C0}=8.5\ \mu$A which is carried by $N=2W/\lambda_F\simeq 1200$ transport modes we would expect an average critical current step height $\Delta I_C=I_{C0}\lambda_F/2W\simeq 7$ nA, which agrees well with the magnitude of the critical current quantization observed here.

VI. CONCLUSION

We have measured the conductance and supercurrent of a S-2DEG-S Josephson junction SQPC. Both the conductance and the supercurrent showed a steplike structure as a function of gate voltage. Unlike the data presented in Ref. 9 we observed that the steps in the supercurrent and the conductance are correlated. Furthermore, we could see evidence of a critical current in the SQPC which was carried by the first open transport mode in the SQPC. We could fit the gate voltage dependence of the critical current and conductance with parameters typical for our junction.

ACKNOWLEDGMENTS

We would like to acknowledge stimulating discussions with N. Chtchelkatchev, V. Shumeiko, and F. Lombardi. This work was supported by the Japanese NEDO, G. Gustavsson foundation and Deutsche Forschungsgemeinschaft.

*Electronic address: thilo.bauch@mc2.chalmers.se

[1] B. J. van Wees, H. van Houten, C. W. J. Beenakker, J. Williamson, L. Kouwenhoven, D. van der Marel, and C. Foxton, Phys. Rev. Lett. **60**, 848 (1988).
[2] D. Wharam, T. Thornton, R. Newbury, M. Pepper, H. Ahmed, J. Frost, D. Hasko, D. Peacock, D. Ritchie, and G. Jones, J. Phys. C **21**, L209 (1988).
[3] C. W. J. Beenakker and H. van Houten, Phys. Rev. Lett. **66**, 3056 (1991).
[4] A. Furusaki, H. Takayanagi, and M. Tsukada, Phys. Rev. Lett. **67**, 132 (1991).
[5] A. Furusaki, H. Takayanagi, and M. Tsukada, Phys. Rev. B **45**, 10 563 (1992).
[6] N. M. Chtchelkatchev, G. B. Lesovik, and G. Blatter, Phys. Rev. B **62**, 3559 (2000).
[7] N. Shchelkachev, JETP Lett. **71**, 504 (2000).
[8] C. J. Muller, J. M. van Ruitenbeek, and L. J. de Jongh, Phys. Rev. Lett. **69**, 140 (1992).
[9] H. Takayanagi, T. Akazaki, and J. Nitta, Phys. Rev. Lett. **75**, 3533 (1995).
[10] I. Kulik and A. Omelyanchuk, Sov. J. Low Temp. Phys. **4**, 142 (1978).
[11] R. Landauer, IBM J. Res. Dev. **1**, 223 (1957).
[12] R. Landauer, Philos. Mag. **21**, 863 (1970).
[13] G. E. Blonder, M. Tinkham, and T. M. Klapwijk, Phys. Rev. B **25**, 4515 (1982).
[14] T. Akazaki and H. Takayanagi, Jpn. J. Appl. Phys., Part 1 **34**, 6977 (1995).
[15] K. Bladh, D. Gunnarson, E. Hürfeld, S. Devi, C. Kristofferson, B. Smalander, S. Pehrson, T. Claeson, and P. Delsing, Rev. Sci. Instrum. **74**, 1323 (2003).
[16] A. Zorin, Rev. Sci. Instrum. **66**, 4296 (1995).
[17] V. Ambegaokar and B. Halperin, Phys. Rev. Lett. **22**, 1364 (1969).
[18] M. Octavio, M. Tinkham, G. E. Blonder, and T. M. Klapwijk, Phys. Rev. B **27**, 6739 (1983).